processes

MDPI

Article

Synthesis and Characterization of Nanoformulation of the Broad-Spectrum Enzyme Inhibitor Mancozeb by Polyethylene Glycol Capping and Its Dissipation Kinetics in Water Using TiO_2 Nanoparticles

Wafa Mahmoud Daqa [1,*], Adil Alshoaibi [1,*], Faheem Ahmed [1] and Tentu Nageswara Rao [2]

[1] Department of Physics, College of Science, King Faisal University, P.O. Box 400, Al Ahsa 31982, Saudi Arabia
[2] Department of Chemistry, Krishna University, Machilipatnam 521003, India
* Correspondence: wdakkah@kfu.edu.sa (W.M.D.); adshoaibi@kfu.edu.sa (A.A.)

Abstract: The poly(ethylene) glycol (PEG) capped mancozeb nanoformulation was prepared by the ultrasonic method using a 1% mancozeb solution and 20% capping agent, PEG-4000. The synthesized nanoformulation was characterized using UV-visible, FTIR, SEM and TEM techniques. The photolytic and photo catalytic experiments were carried out in a Borosil glass bottle in the presence of sunlight, varying the pH proportions at a single fortification level (1.0 g/mL) in ground water, under sunlight. The optimal catalyst concentration for complete degradation was observed to be 0.1 percent. The mancozeb nanoformulation in water was determined using the HPLC-PDA method, and the rate constant and the 50% degradation (DT50) values were calculated based on the results. The photolytic results show that there is no significant loss of residues due to adsorption. Titanium dioxide (TiO_2) was discovered to be an excellent decontaminating catalyst in a variety of water samples. The compound survives for several days in the absence of a catalyst.

Keywords: mancozeb nanoformulation; polyethylene glycol; TiO_2 nanoparticles; photolytic; photocatalytic; dissipation half-life (DT50)

Citation: Daqa, W.M.; Alshoaibi, A.; Ahmed, F.; Rao, T.N. Synthesis and Characterization of Nanoformulation of the Broad-Spectrum Enzyme Inhibitor Mancozeb by Polyethylene Glycol Capping and Its Dissipation Kinetics in Water Using TiO_2 Nanoparticles. *Processes* **2022**, *10*, 2733. https://doi.org/10.3390/pr10122733

Academic Editors: María Victoria López Ramón and Andrea Petrella

Received: 5 October 2022
Accepted: 15 December 2022
Published: 18 December 2022

1. Introduction

Dithiocarbamate fungicides (DTCs) have been widely used on a variety of crops around the world due to their broad spectrum control of a wide range of fungal diseases. Following their transformation into water soluble sodium salts with an aqueous alkaline ethylenediaminetetraacetic acid (EDTA) solution, DTCs are frequently methylated with methyl iodide [1–4]. Mancozeb (MCZ) is a fungicide that is effective against a wide variety of fungi. It interferes with sulphydryl containing enzymes and disrupts many essential enzymatic processes. Although its half-life is 1–7 days, the primary metabolite ethylenethiourea (ETU) has the potential to contaminate ground water [5]. Mancozeb is a water-soluble, non-systemic contact fungicide with the disadvantage of polluting bodies of water. Biopolymers are ideal carriers for plant ingredients due to their biocompatibility and ability to encapsulate a wide range of compounds [6–9]. Health and environmental concerns have prompted governments around the world to consider limiting pesticide use. Pesticide residue research helps with crop protection, environmental monitoring, consumer protection, and legislative enforcement. In Uganda, there is insufficient scientific evidence to support interventions spanning the entire chemical management life cycle. There have been allegations of substance abuse and misuse of Mancozeb in post-harvest applications to extend fruit shelf life [10–12]. Most fungicides have been encapsulated using nanoformulations of pesticides based on polymers [13–15]. Because of the properties and multifunctional structures of each segment, there have been few studies on polymer nano composites. Nanoparticles describe the possibilities for pest control, but our lack of

knowledge about how they act and how they can be contained is preventing regulators from allowing their release [16]. The encapsulation of most insecticides has been achieved using nanoformulations of pesticides based on polymers [17]. The encapsulation process has wide applications, such as for foods, cosmetics, paints, paper, textiles etc. The first polymer-containing formulation was developed in the year 1970 for the controlled release of biocides [18]. Due to its fungicidal and fungistatic potential against plant pathogens, many researchers have identified it as a plant growth promoter and anti-fungal agent as well as its ability to elicit defense-related enzymes in cereals and horticultural crops. Health and environmental concerns have prompted authorities all over the world to consider limiting or prohibiting the use of many current pesticides, resulting in a search for safe substitutes for pest and other agricultural insect control [19–21]. Fungicide nano encapsulation in biopolymers, such as chitosan and gum acacia, has been applied to commercial fungicides and has the potential to improve disease potency through controlled release, site-directed delivery, and reduced toxicity [22]. The poly(ethylene) glycols (PEG) based polymers used for encapsulation are environmentally friendly, cost-effective, nontoxic, biocompatible, and long-lasting, with a wide range of solubilities, and can be easily modified or linked with other polymers [23–25]. Titania, which exists as titanium oxide, is recognized as nanoparticles (NPs) of metal oxides. TiO_2 has distinct optical, thermal, electrical, and magnetic properties. Photocatalytic degradation and splitting, PV cells, electrochromic and electronic devices, and sensing instruments are all critical applications of nano TiO_2. It is a naturally occurring oxide form of titanium metal that can be obtained from minerals such as anatase, rutile, or brookite. The photocatalytic activity of titania depends on the crystal phase, particle size and degree of crystallinity. TiO_2 has unique properties, such as easy control, low cost, non-toxicity, and high resistance to chemical erosion. It is widely used as a pigment in plastics, paints, inks, paper, food coloring, food additives, and cosmetics. Plants, soil, microorganisms, and other environmental factors are affected by nanoparticles in both positive and negative ways [26–28]. Photocatalysis has been investigated extensively in order to efficiently convert light energy into reliable and efficient chemical energy. Unilamellar liposomes and nanocapsules are the most common drug delivery systems. The former are vesicles with phospholipid membranes that have been extensively described in literature. The latter are made up of a small solid or liquid core surrounded by a thin water-insoluble membrane [29]. Photocatalytic degradation is becoming increasingly important in wastewater treatment [30–32]. The mineralization of carbon dioxide, water, and simple mineral acids can result in the formation of hazardous organic chemicals. Photocatalysts can be reused or recycled, and they can also regenerate themselves [33–36]. With this motivation, we investigated the dissipation activity of mancozeb nanoformulation in three different pH waters using TiO_2 nanoparticles as a photo catalyst in UV visible sunlight under natural climate conditions.

2. Materials and Methods

2.1. Equipment Details

Mancozeb residues were analyzed using Zorbax Eclipse C18 (250 × 4.6 mm, 5 µm) column, high performance liquid chromatography (HPLC), Agilent with DAD detector, and interfaced with openlab solutions software. M/s Fourier transform infrared (FTIR) spectroscopy Agilent cary 630 (Santa Clara, CA, USA) for the characterizations of TiO_2 nanoparticles and mancozeb nanoformulations, scanning electron microscope (SEM), transmission electron microscope (TEM) and X-Ray diffraction (XRD) were also used for nanoparticle and nanoformulation characterization. The analytical balance from Shimadzu was used to weigh the samples.

2.2. Reagents and Chemicals

Sigma Aldrich (St. Louis, MO, USA) provided Manocozeb technical (purity 85%), titanium tetrachloride, and iron nitrate. Merck Ltd. (Rahway, NJ, USA) supplied the polyethylene glycol, potassium dihydrogen orthophosphate, and EDTA. Merck India

limited provided acetonitrile, water HPLC grade, sodium hydroxide LR grade, potassium chloride GR grade, boric acid GR grade, potassium biphthalate GR grade, hydrochloric acid AR grade, and potassium phosphate AR grade. The Milli-Q Plus apparatus was used to purify distilled water (Millipore, Bedford, MA, USA). RO water used from in house plant.

3. Experimental

The quantity of about 1 g of mancozeb technical fine powder was weighed into a mortar. We added 5 mL of RO water into the mortar and triturated well. The contents were transferred into a 500 mL glass beaker and the volume was made up to 200 mL mark with RO water and mixed well. Subsequently, 200 mL 3% polyethylene glycol (PEG-4000) was added in portions to the same glass beaker. The solution was sonicated up to 30 min using an ultrasonic bath, then the solution was continuously stirred for 12 h at 1000 rpm. After that, the solution was covered with aluminum foil and kept stable overnight. The mixture solution was changed from a yellow color to brown color. It indicates the formation of mancozeb nano-formulation.

3.1. Preparation of TiO_2 Nanoparticles

We prepared the TiO_2 nanoparticles by adding drop-wise 4 mL of titanium tetrachloride ($TiCl_4$) in 100 mL distilled water containing 0.1 M hydrochloric acid (HCl) at 55 °C, ultrasonicating for one hour at 75 °C, and then keeping them at 75 °C for 12 h under a thermostat:

$$TiCl_4 + 2\,H_2O \longrightarrow TiO_2 + 4\,HCl \quad (1)$$

A precipitate of TiO_2 nanoparticles was obtained by decanting distilled water into a glass container and drying the precipitate for five hours at 300 °C.

3.2. Preparation of 25 mm EDTA Stock Solution (Diluent)

EDTA of 9.8 g was taken and dissolved with 1000 mL of Milli-Q water, sonicated. We used milli-Q water to make up the volume to 1000 mL.

3.3. Preparation of 100 mM Potassium Dihydrogen Orthophosphate Solution Stock

Potassium dihydrogen orthophosphate of 0.35 g was taken and dissolved with 25 mL of Milli-Q water, sonicated. The volume was made up to 25 mL with milli-Q water.

3.4. Preparation of 1,2 Benzene Dithiol Solution Stock

Then, 1,2 benzene dithiol of 28.07 mg was taken in 20 mL volumetric flask and 5 mL of isopropanol was added and sonicated. The volume was made up to 10 mL by using isopropanol.

3.5. Preparation of Mancozeb Standard Stock Solution

Accurately, 20.05 mg of mancozeb reference standard was weighed into a 20 mL volumetric flask, adding 5 mL of diluent, and sonicated until the content dissolved. Finally, we filled up to the mark with the same diluent. Further, 0.5 mL of standard stock was mixed with 0.5 mL of 25 mM EDTA, then 300 µL of potassium dihydrogen orthophosphate and 500 µL of 1,2-benzene dithiol was added. It was incubated at 60 °C for 2 h and cooled to room temperature. Isopropanol was added to make up the volume and incubated for an additional 2 h.

3.6. Effect of Catalyst Amount

To investigate the effect of TiO_2 amount on the decontamination of pesticide in water, water was spiked with 1 mL of 1000 mg/L stock solution of pesticide formulation to obtain 1 µg/mL concentration of pesticide active in water (each pesticide was spiked into a separate one-liter glass bottle) and was loaded TiO_2 by varying the amount of 0, 0.01, 0.05, 0.10, 0.20 and 0.50 g/L in water (separate one-liter glass bottles were maintained for each amount of TiO_2). The samples were sonicated in the dark for 10 min prior to exposure

to the sun in order to achieve the adsorption equilibrium and an even dispersion of TiO_2 particles in water. During the day, the bottles were exposed to the sun from 8 a.m. until the evening at 5 p.m. on 22 August 2022.

3.7. Photolysis and Photocatalytic Studies

The photolysis and photocatalysis of mancozeb nanoformulation in ground water were studied by spiking the mancozeb nanoformulation at 1 mg L^{-1} level. The study was conducted in ground water. Two sets were made at 1 mg L^{-1} fortification level along with control samples for comparison. The catalyst (0.1 g/L TiO_2 NPs) was added to one set of the sample, and no catalyst was added to the other set. The samples were exposed to direct sunlight. Aliquots of samples were collected on pre-determined intervals. The temperature of the water samples during the period was 20 to 45 °C. Samples were extracted from 0.2 m PTFE membrane filters and filtered in amber-colored vials with 0.2 m PTFE membrane filters. All the samples were stored in the dark at <5 °C before subjecting to HPLC-DAD analysis. The samples fortified with TiO_2 nano catalyst were centrifuged using Beckman cooling centrifuge at 10,000 rotations per minute for 4 min at 5 °C. We transferred the supernatant to the amber-colored bottles and stored them in the dark at <5 °C until analysis to avoid further degradation of the residues. The intensity of the sunlight and temperature were measured during the exposure time using LUX meter.

3.8. Sampling Data

Water samples were collected from the bottle at different depths at different occasions after exposure under sunlight (0.4, 3, 6, 12, 24 and 36 h for photocatalytic experiment and 0, 5, 10, 15, 20 and 30 days for photolytic experiment). The collected water sample was centrifuged and filtered thoroughly 0.20 µ filter and analysed in HPLC.

3.9. Chromatographic Separation Parameters

Residue quantification was performed using an Agilent series high performance liquid chromatography (HPLC) equipped with a diode array detector. The wavelength of the detector was set to 365 nm. Herbicide residues were separated using the Agilent Zorbax Eclipse C18 (250 × 4.6 mm, 5 µm). The mobile phase used was (ACN: HPLC grade water, 80:20 v/v). The flow was programmed, and a 1.0 mL per minute flow rate was set. The injection volume 20 µL was set for standard and sample. Mancozeb was eluted about 5.2 min.

3.10. Characterization

Using an X-ray diffractometer (Philips X'Pert; MPD 3040, EA Almelo, The Netherlands) outfitted with Cu Kα radiations in the 2 range of 10–85°, the structural characteristics of the samples were determined. The sample's crystal structure and phase purity were examined, and the "Debye Scherrer" equation was used to compute the crystallite size from the XRD patterns. The surface morphology of TiO_2 NPs and mancozeb nanoformulation was investigated using SEM (TESCAN, CZ/MIRA I LMH). The particle size and shape were studied using TEM (FEI, TECNAI G2 TF20-ST). A JASCO FT/IR-6300 FT-IR spectrometer was used to record the infrared transform (FT-IR) spectra in KBr pellets.

4. Results and Discussion

4.1. Characterization of TiO_2 NPs and Mancozeb Nanoformulation

4.1.1. XRD Analysis of TiO_2

Figure 1 shows the XRD patterns of TiO_2. It is found that all of the crystal phase is anatase for the sample. The shape of the diffraction peaks of all the photo catalysts was consistent with that of TiO_2. About 25°, 38°, 48°, 54°, 62°, 68°, 74°, and 82° are the well-defined diffraction peaks with 2, which are ascribed to the crystal planes (101), (004), (200), (211), (116), (220), (215), and (224), respectively. This XRD characteristic pattern is

compatible with the typical JCPDS values of tetragonal-structured anatase TiO_2 (JCPDS Card No. 21-1272), which did not occur in rutile or brookite form.

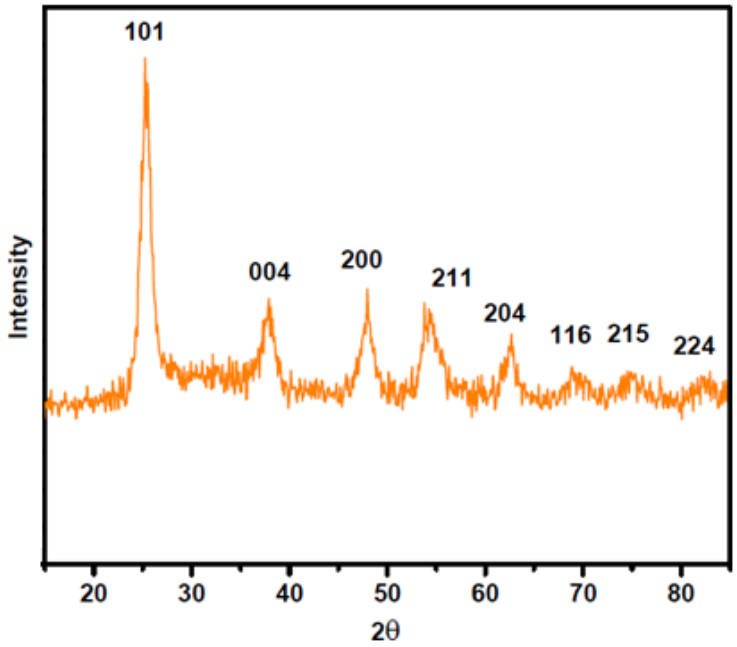

Figure 1. X-Ray diffraction pattern of TiO_2 nanoparticles.

4.1.2. FTIR Analysis TiO_2 NPs and Mancozeb Nanoformulation

The FTIR spectrum of the TiO_2 in the frequency range of 500–4000 cm^{-1} is shown in Figure 2. The sample exhibits peaks corresponding to the O–H stretching vibration of the TiO_2 NPs and the bending vibrations of the adsorbed water molecules at wavelengths of 3400 cm^{-1} and 1630 cm^{-1}, respectively. Furthermore, the broadening of ~3400 cm^{-1} O–H stretching vibration the formation of a different –OH group, and most probably as Ti–OH surface group. The Ti–O (600 cm^{-1}) stretching and Ti–O–Ti bridging stretching modes are responsible for the broad intensity band between 450 and 700 cm^{-1}.

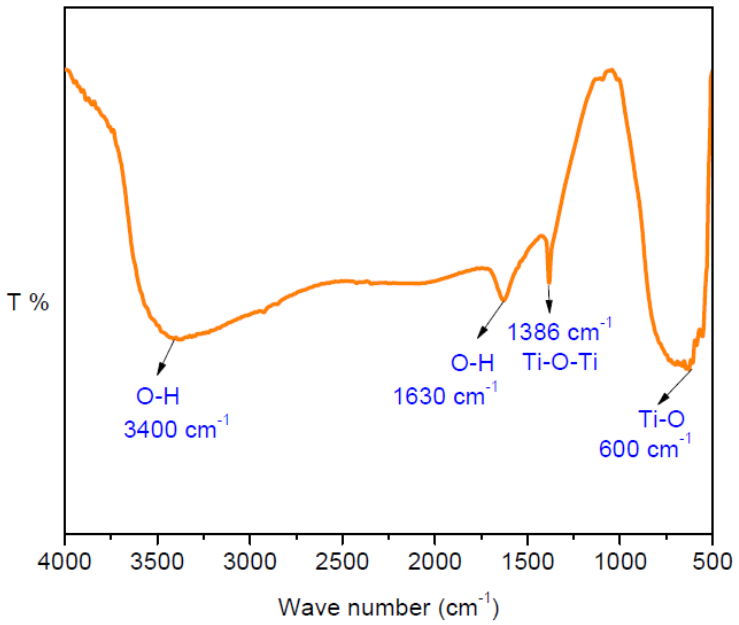

Figure 2. FTIR spectrum of TiO_2 nanoparticles.

FTIR spectral analysis of synthesized mancozeb formulation was recorded using a FTIR spectrophotometer within the range of 650–4000 cm^{-1}. It is a KBr analytical characterization technique. FTIR to identify the characteristic spectra of mancozeb (Figure 3). The strong intense and medium-weak bonds were observed at 1515 cm^{-1} and 1390 cm^{-1} which shows the presence of a triazine ring and C_3N_3 bond stretching. The strong stretching of NH bond at 3283 cm^{-1} and deformation of NH bond at 1515 cm^{-1} and 760 to 680 cm^{-1} was also observed for mancozeb.

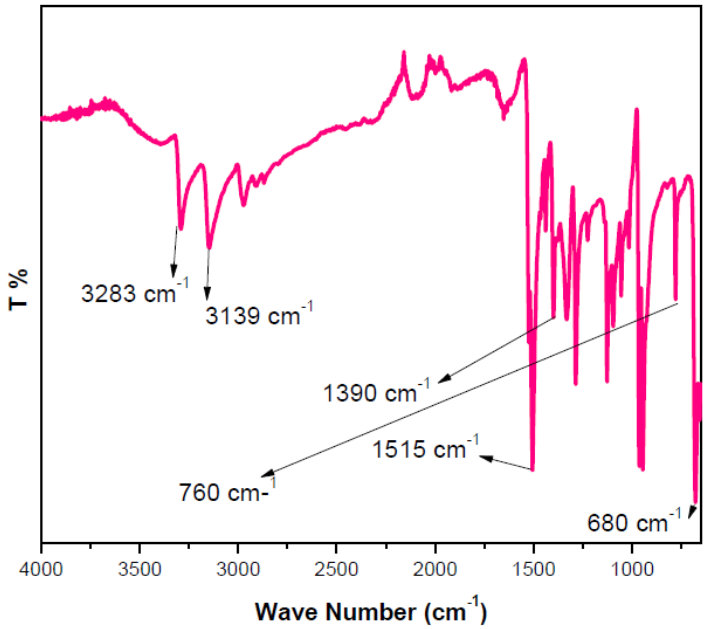

Figure 3. FTIR spectrum of mancozeb nanoformulation.

4.1.3. SEM Analysis of TiO_2 NPs and Mancozeb Nanoformulation

According to the SEM, the morphology of the TiO_2 nanoparticles were observed and approximately spherical, TiO_2 nanoparticles were in an aggregated form. This reveals that the powder particles are slightly agglomerated, and the closed view of spherical nanoparticles is shown (Figure 4). The SEM micrograph revealed the presence of particles with irregular shapes and sizes (Figure 5). Furthermore, in some regions, the interconnectivity of the particles increased, which has given rise to agglomerated regions within the sample. Thus, it is speculated here that some particles within the sample act as a nucleation center around which the condensation of the smaller particles occurs, and hence gives rise to agglomeration.

4.1.4. TEM Analysis of TiO_2 NPs and Mancozeb Nanoformulation

The particle size, crystallinity, and morphology of the samples were examined using transmission electron microscopy. The main objective of TEM is to describe an item individually, rather than in bulk. It is used to precisely analyze particles and particle boundaries. The TEM image in Figure 6a shows the high resolution morphology of the nanostructured particles containing anatase TiO_2 that were calcined at 300 °C. Titania was found to be virtually entirely constituted of tiny sized nano crystallites. The TEM image clearly shows that the individual nanoparticles generated are virtually spherical in shape and range in size from 10 to 50 nm as shown in Figure 6b. The TEM image of the mancozeb nanoformulation is shown in Figure 7a. The particles appeared to have different shapes and sizes in the TEM image. From Figure 7b, we can see that the particle size was close to 20 to 50 nm.

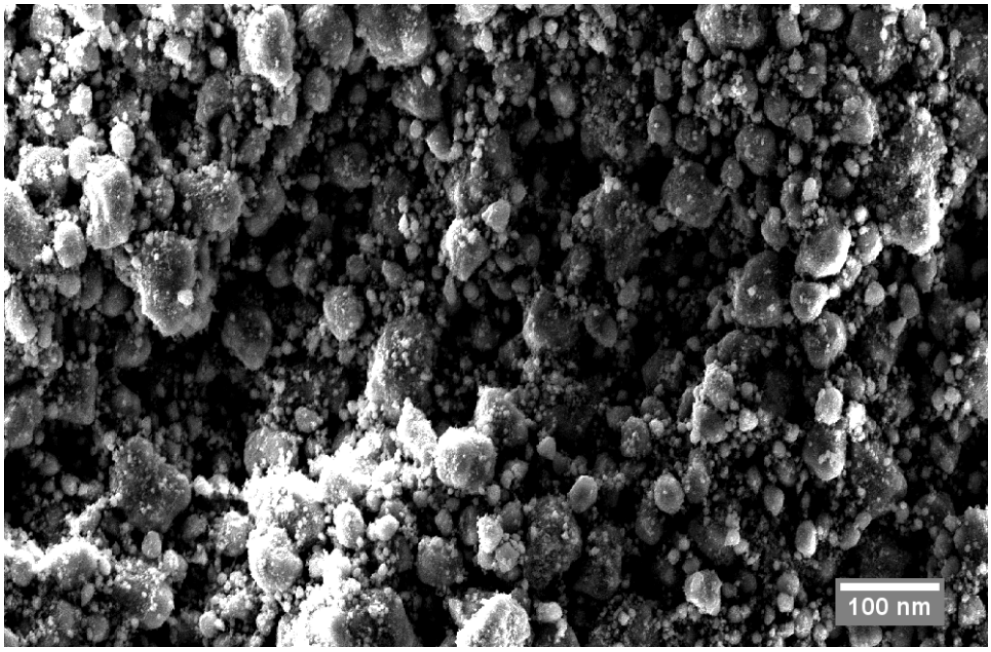

Figure 4. SEM image of TiO_2 nanoparticles.

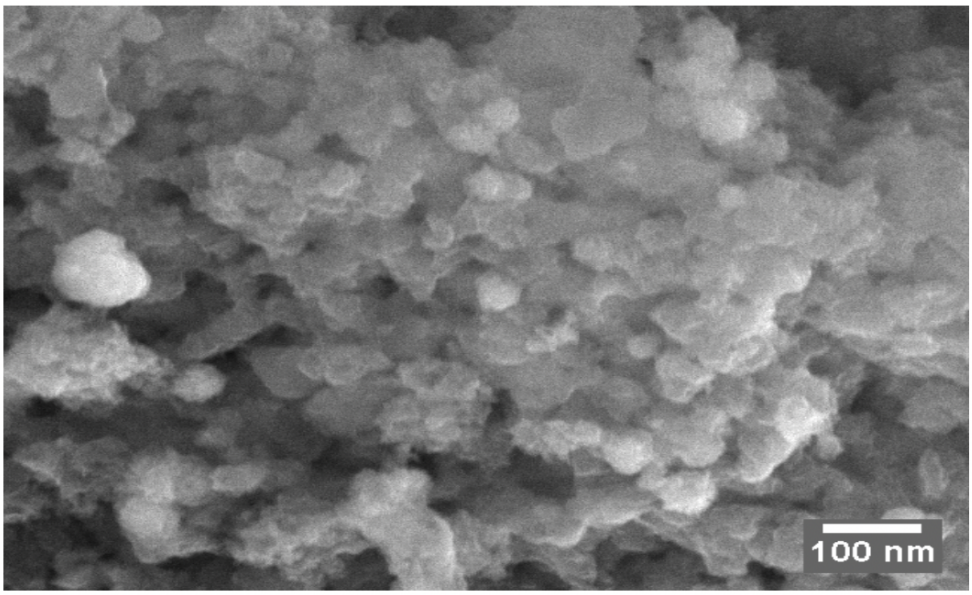

Figure 5. SEM image of mancozeb nanoformulation.

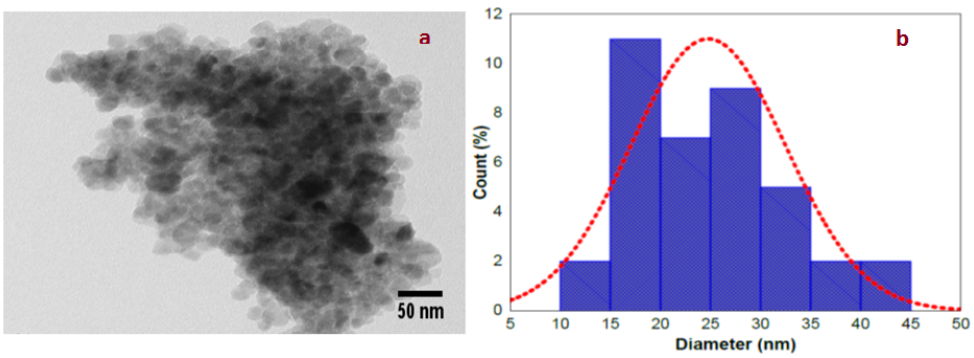

Figure 6. (**a**) TEM image of TiO_2 nanoparticles and (**b**) size distribution curve.

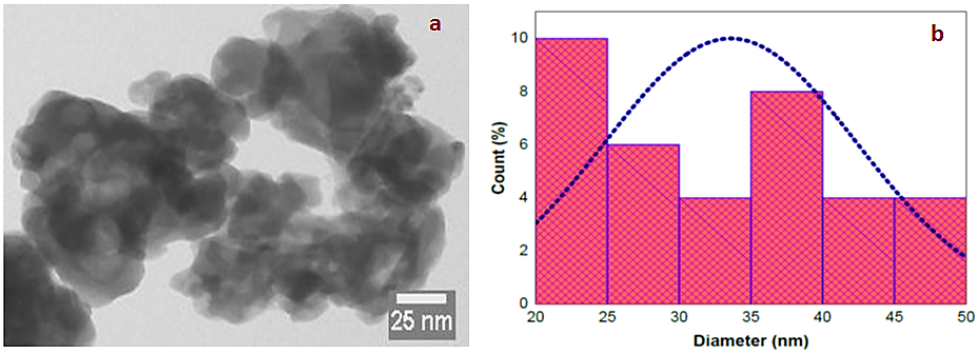

Figure 7. (**a**) TEM image of mancozeb nanoformulation and (**b**) size distribution curve.

4.2. Effect of Catalyst Amount

To determine the effective amount of catalyst for rapid degradation of pesticide in water on the photocatalytic decontamination, experiments were carried out by varying the amount of TiO_2 in water from 0.01 to 0.5 g/L. From the experimental results, it was observed an acceleration in the photocatalytic decontamination rate with an increase in concentration from 0.01 to 0.1 g/L, whereas no increase in the rate was observed when the concentration of the TiO_2 was increased above 0.1 g/L. The summarized results for effect of catalyst amount are presented in Table 1 and Figure 8. With 0.1 g/L of catalyst, recovery studies in water and various buffers were carried out. The adsorption of residues on the catalyst was evaluated by measuring the concentration of mancozeb in water over a three-hour period. In acidic water, neutral water, and basic water, the recovery rates were 90 to 93%, 91 to 95%, and 91 to 96%, respectively. The findings clearly show that there is no significant loss of residues due to adsorption.

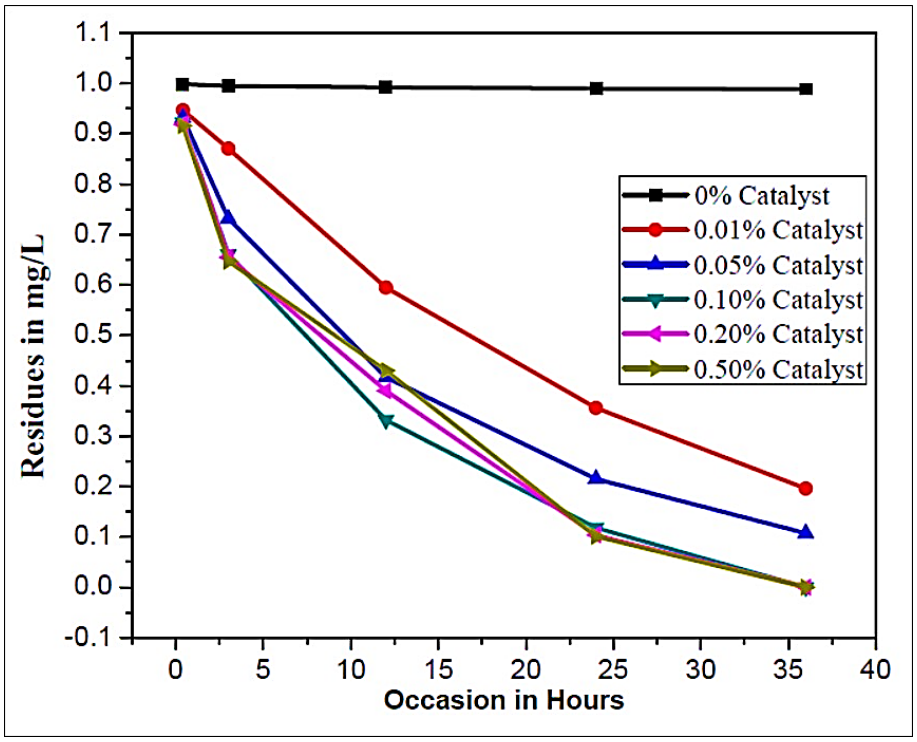

Figure 8. Plot representing the effect of catalyst amount on decontamination of mancozeb in water under direct sunlight.

Table 1. Dissipation data for effect of catalyst amount on decontamination of nanoformulation in water under direct sunlight.

Occasion (Hours)	Nanoformulation Residues (mg/L)					
	0 g/L Catalyst	0.01 g/L Catalyst	0.05 g/L Catalyst	0.10 g/L Catalyst	0. 20 g/L Catalyst	0.50 g/L Catalyst
0.4	0.999	0.947	0.932	0.923	0.919	0.916
3	0.995	0.871	0.732	0.661	0.655	0.647
12	0.992	0.595	0.417	0.332	0.39	0.43
24	0.990	0.356	0.215	0.118	0.104	0.101
36	0.989	0.196	0.107	ND	ND	ND

ND: not detected.

4.3. Photolysis and Photocatalytic Studies

The photolytic degradation results of mancozeb nanoformulation in water showed that the residues are highly stable. The half-life of nanoformulation was 7.77 days in water without catalyst. The summarized results such as kinetic parameters rate constant (k) and DT50 for photolytic studies are presented in Table 2 and Figure 9. Whereas the half-life of mancozeb nanoformulation in the presence of a catalyst in water was recorded to be 8.30 h. The summarized results, such as kinetic parameters rate constant (k) and DT50 for photolytic studies are presented in Table 3 and Figure 10. The data clearly demonstrate that the dissipation of pesticide follows pseudo-first-order kinetics when calculating the residues values with time by using the first-order kinetic formula. The representative photocatalytic 0th hour mancozeb standard, control and sample chromatograms presented in Figure 11. The data clearly show that pesticide decontamination follows pseudo-first-order kinetics in TiO_2-loaded water when residue values are calculated with time using a below-first-order kinetic formula. There were no pesticide residues because no pesticides were used, and there was no degradation of mancozeb in due to TiO_2 inactivation in the absence of light. The pseudo-first-order kinetics form is

$$-\ln \frac{C_t}{C_0} = kt \tag{2}$$

$$t_{1/2} \equiv DT_{50} = \frac{\ln 2}{k} \tag{3}$$

$$k = \frac{2.303}{t} \times \log_{10} \frac{C_0}{C_t} \tag{4}$$

where,

C_0: Pesticide concentration at times zero
C_t: Pesticide concentration at times t,
k: The rate constant.
DT_{50}: Half-life. Kinetic parameters, such as rate constant (k)

When studied under sunlight in the presence of TiO_2 in water, the decontamination was rapid due to the formation of electrons (e^-) and positive holes (h^+) in TiO_2 when it absorbed energy from sunlight, and the availability of electrons (e^-) and positive holes (h^+) pairs that were contributing to the simultaneous oxidation and reduction of pesticide in soil was enhanced by TiO_2. This was confirmed by the absence of pesticide degradation in water samples stored in the dark. Pesticide residues were also absent in water-spiked water samples because no pesticide was used.

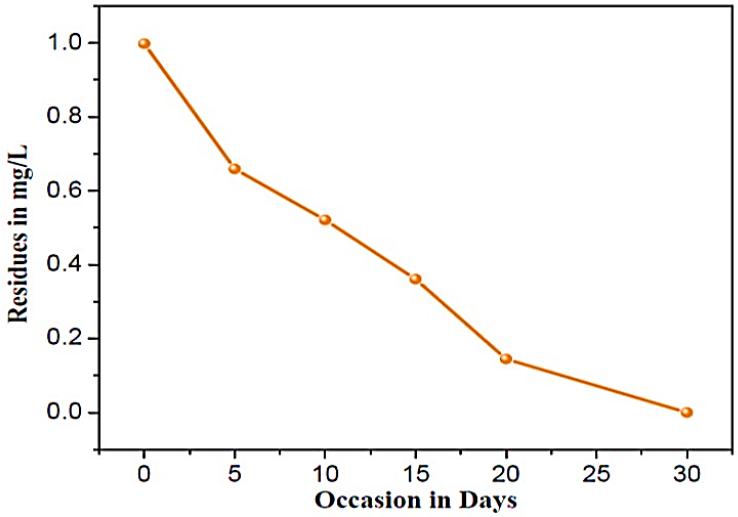

Figure 9. Graph representing the dissipation curve of photolytic decontamination of mancozeb in water under direct sunlight.

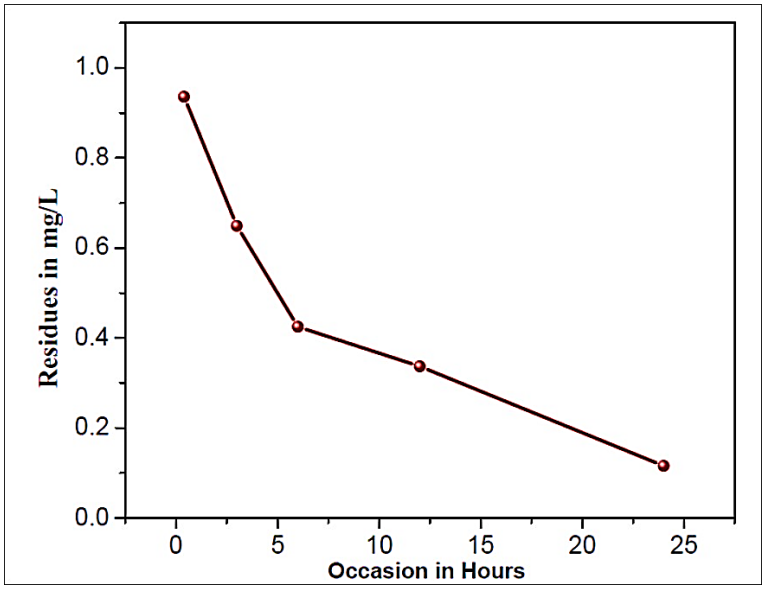

Figure 10. Graph representing the dissipation curve of photocatalytic decontamination of mancozeb in water under direct sunlight.

Table 2. The photolytic summarized results of kinetic parameters.

Occasion (Days)	Residue Level (mg/L)	Log	Kinetic Parameters	
0	0.998	−0.0009		
5	0.659	−0.1811	**Slope**	−0.039
10	0.521	−0.2832	**Half-life (Days)**	7.77
15	0.361	−0.4425	**Intercept**	0.038
20	0.145	−0.8386	**CC**	0.966
30	ND	ND		

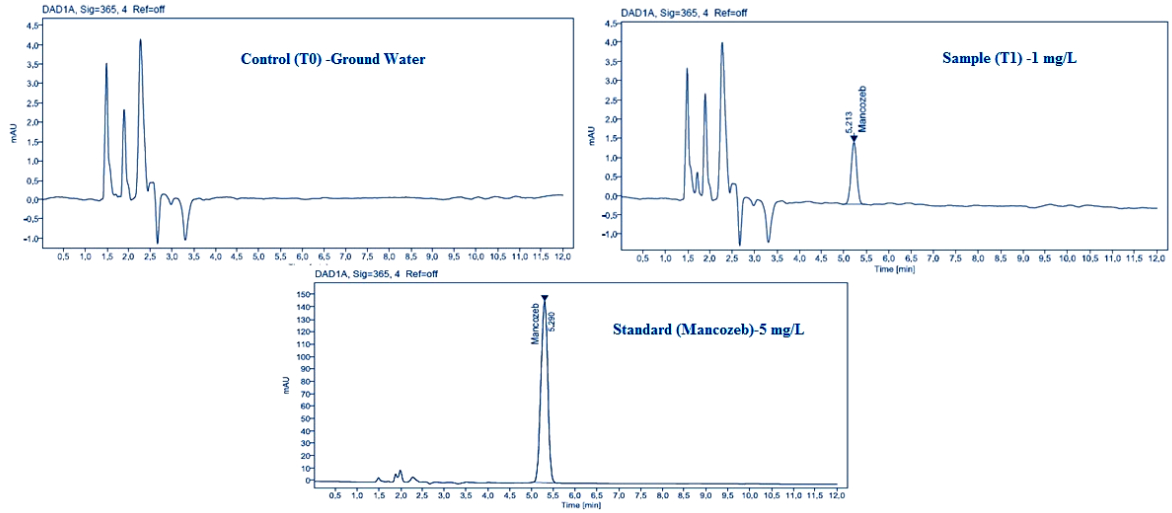

Figure 11. Representative photocatalytic 0th hour mancozeb standard, control and sample chromatograms.

Table 3. The photocatalytic summarized results of kinetic parameters.

Occasion (Days)	Residue Level (mg/L)	Log	Kinetic Parameters	
0.4	0.936	−0.0287		
3	0.649	−0.1878	**Slope**	−0.036
6	0.425	−0.3716	**Half-life (Hours)**	8.30
12	0.337	−0.4724	**Intercept**	−0.070
24	0.116	−0.9355	**CC**	0.988
36	ND	ND		

5. Conclusions

Polyethylene glycol, an additive, is used to reduce the size of pesticide molecules. Nanopesticide is a better alternate pesticide. PEG was used as a capping ingredient in the formulation of mancozeb nanoformulation. TiO_2 nanoparticles have unique properties such as quantum size effect, high surface area, short interface migration distance, and visible light activity, which all contribute to improved photocatalytic performance. Particle size is another important parameter for photocatalysis because it directly affects a catalyst's specific surface area. The number of active surface sites increases with particle size, as does the rate of surface charge carrier transfer in photocatalysis. The photo-catalysis study in water using TiO_2 nanoparticles showed the potential of catalyst in decontamination of residues of mancozeb in water. The amount of catalyst required to decontaminate the residues per liter water is 0.01 to 0.5 % w/v significantly low quantities. The optimal concentration of catalyst was 0.1 % w/v. The photocatalysis studies have been carried out for mancozeb nanoformulation under direct sunlight in water with and without a catalyst in which the best photocatalytic activity was shown by TiO_2 nanoparticles in water with the degradation of mancozeb nanoformulation.

Author Contributions: Conceptualization, W.M.D. and T.N.R.; methodology, T.N.R.; validation, A.A. and F.A.; formal analysis, T.N.R. and F.A.; investigation, W.M.D. and A.A.; resources, A.A. and W.M.D.; data curation, T.N.R. and F.A.; writing—original draft preparation, T.N.R. and W.M.D.; writing—review and editing, W.D, A.A., F.A. and T.N.R.; visualization, W.M.D. and A.A.; supervision, A.A.; project administration, A.A. and W.M.D.; funding acquisition, W.M.D. All authors have read and agreed to the published version of the manuscript.

Funding: This research was funded by the Deanship of Scientific Research, Vice Presidency for Graduate Studies and Scientific Research, King Faisal University, Saudi Arabia [Grant No. 1327], through its KFU Research Summer initiative.

Data Availability Statement: Available on request.

Acknowledgments: The authors would like to thank the Deanship of Scientific Research, Vice Presidency for Graduate Studies and Scientific Research, King Faisal University, Saudi Arabia for supporting this research.

Conflicts of Interest: The authors declare no conflict of interest.

References

1. Anitha, S.R.; Savitha, G. Impact of Mancozeb Stress on Seedling growth, Seed Germination, Chlorophyll and Phenolic Contents of Rice Cultivars. *Int. J. Sci. Res.* **2015**, *4*, 292–296.
2. Sayed, R.; Hussein, O.E.; Omran,A.A. Method optimization and validation for the determination of mancozeb in chamomile by modified QuEChERS and liquid chromatography–tandem mass spectrometry. *J. Food Compos. Anal.* **2022**, *111*, 104646. [CrossRef]
3. Venugopal, N.V.S.; Sainadh, N.V.S. Novel polymeric nanoformulation of mancozeb—An eco-friendly nanomaterial. *Int. J. Nanosci.* **2016**, *15*, 1650016. [CrossRef]
4. Marinas, M.; Sa, E.; Rojas, M.M.; Moalem, M.; Urbano, F.J.; Guillou, C.; Rallo, L. A nuclear magnetic resonance (^{1}H and ^{13}C) and isotope ratio mass spectrometry (δ^{13}C, δ^{2}H and δ^{18}O) study of Andalusian olive oils. *Rapid Commun. Mass Spectrom.* **2010**, *24*, 1457–1466.
5. Huang, Z.; Wang, P.; Pu, Z.; Lu, L.; Chen, G.; Hu, X.; Fayyaz, A.; Gai, Y. Effects of mancozeb on citrus rhizosphere bacterial community. *Microb. Pathog.* **2021**, *154*, 104845. [CrossRef]
6. Shim, Y.-S.; Yoon, W.-J.; Hwang, J.-B.; Park, H.-J.; Seo, D.; Ha, J. Rapid method for the determination of 14 isoflavones in food using UHPLC coupled to photo diode array detection. *Food Chem.* **2015**, *187*, 391–397. [CrossRef]
7. Gullino, M.L.; Tinivella, F.; Garibaldi, A.; Kemmitt, G.M.; Bacci, L.; Sheppard, B. Mancozeb: Past, present, and future. *Plant Dis.* **2010**, *94*, 1076–1087. [CrossRef]
8. Nikunj, P.; Purvi, D.; Niti, P.; Anamika, J.; Gautam, H.K. Agronanotechnology for plant fungal disease management: A review. *Int. J. Curr. Micobl. App. Sci.* **2014**, *3*, 71–84.
9. Wang, X.; Peng, F.; Cheng, C.; Chen, L.; Shi, X.; Gao, X.; Li, J. Synergistic antifungal activity of graphene oxide and fungicides against Fusarium head blight in vitro and in vivo. *Nanomaterials* **2021**, *11*, 2393. [CrossRef]
10. Court, R. *Agency Technical Report on the Classification and Labelling of Mancozeb (ISO); Manganese Ethylenebis(dithiocarbamate) (Polymeric) Complex with Zinc Salt*; CAS Number: 8018-01-7; Health and Safety Executive Chemicals Regulation Division: Bootle, UK, 2021.
11. Debelder, T. *Mancozeb Non-Renewal and MRL Review (Voluntary Report)*; E42020-0099; USDA, United States Department of Agricultural Service: Washington, DC, USA, 2020.
12. ANZG A Toxicant default guideline values for aquatic ecosystem protection—Metolachlor in freshwater (Technical brief). In *Australian and New Zealand Guidelines for Fresh and Marine Water Quality*; Australian Government Department of Agriculture, Water and the Environment: Canberra, Australia, 2020.
13. Khay, S.; Abd El-Aty, A.; Choi, J.-H.; Shin, E.-H.; Shin, H.-C.; Kim, J.-S.; Chang, B.-J.; Lee, C.-H.; Shin, S.-C.; Jeong, J.Y.; et al. Simultaneous determination of pyrethroids from pesticide residues in porcine muscle and pasteurized milk using GC. *J. Sep. Sci.* **2009**, *32*, 244–251. [CrossRef]
14. Kakitani, A.; Yoshioka, T.; Nagatomi, Y.; Harayama, K. A rapid and sensitive analysis of dithiocarbamate fungicides using modified QuEChERS method and liquid chromatography–tandem mass spectrometry. *J. Pestic. Sci.* **2017**, *42*, 145–150. [CrossRef] [PubMed]
15. El-Gohary, A.A.; Moustapha, M.; Hassan, A. Method validation of dithiocarbamates residues on some Egyptian commodities using Gc-Mass instrument. *J. Plant Prot. Pathol.* **2011**, *2*, 59–65. [CrossRef]
16. Kumar, R.; Duhan, J.S.; Manuja, A.; Kaur, P.; Kumar, B.; Sadh, P.K. Toxicity Assessment and Control of Early Blight and Stem Rot of *Solanum tuberosum* L. by Mancozeb-Loaded Chitosan–Gum Acacia Nanocomposites. *J. Xenobiot.* **2022**, *12*, 74–90. [CrossRef] [PubMed]
17. Ramesh, A.; Ravi, P.E. Electron ionization gas chromatography–mass spectrometric determination of residues of thirteen pyrethroid insecticides in whole blood. *J. Chromatogr. B* **2004**, *802*, 371–376. [CrossRef] [PubMed]
18. Mujawar, S.; Utture, S.C.; Fonseca, E.; Matarrita, J.; Banerjee, K. Validation of a GC–MS method for the estimation of dithiocarbamate fungicide residues and safety evaluation of mancozeb in fruits and vegetables. *Food Chem.* **2014**, *150*, 175–181. [CrossRef]
19. Saha, N.C.; Giri, S.K.; Chatterjee, N.; Biswas, S.J.; Bej, S. Acute toxic effects of mancozeb to fish Oreochromis mossambicus (WKH Peters, 1852) and their behaviour. *Int. J. Adv. Res. Biol. Sci.* **2016**, *3*, 40–44.
20. Debbarh, I.; Titier, K.; Deridet, E.; Moore, N. Identification and quantitation by high-performance liquid chromatography of mancozeb following derivatization by 1, 2-benzenedithiol. *J. Anal. Toxicol.* **2004**, *28*, 41–45. [CrossRef]

21. Kaye, E.; Nyombi, A.; Mutambuze, I.L.; Muwesa, R. Mancozeb residue on tomatoes in Central Uganda. *J. Health Pollut.* **2015**, *5*, 1–6. [CrossRef]
22. Swarupa, C.; Dhananjayulu, M.S.P.M.; Sreedhar, N. Electrochemical determination and reduction behaviour of mancozeb at glassy carbon electrode modified with polyaniline based nanosensors. *J. Health Pollut.* **2013**, *4*, 1234–1241.
23. Verma, V.; Al-Dossari, M.; Singh, J.; Rawat, M.; Kordy, M.G.; Shaban, M. A Review on Green Synthesis of TiO_2 NPs: Photocatalysis and Antimicrobial Applications. *Polymers* **2022**, *14*, 1444. [CrossRef]
24. Nyamukamba, P.; Okoh, O.; Mungondori, H.; Taziwa, R.; Zinya, S. Synthetic Methods for Titanium Dioxide Nanoparticles: A Review. In *Titanium Dioxide—Material for a Sustainable Environment*; Yang, D., Ed.; IntechOpen: London, UK, 2018; pp. 152–175.
25. Zoccal, J.V.M.; Arouca, F.O.; Gonçalves, J.A.S. Synthesis and Characterization of TiO_2 Nanoparticles by the Method Pechini. *Mater. Sci. Forum (MSF)* **2010**, *660–661*, 385–390. [CrossRef]
26. Bagheri, S.; Shameli, K.; Abd Hamid, S.B. Synthesis and characterization of anatase titanium dioxide nanoparticles using egg white solution via Sol-Gel method. *J. Chem.* **2013**, *2013*, 848205. [CrossRef]
27. Irshad, M.A.; Nawaz, R.; ur Rehman, M.Z.; Adrees, M.; Rizwan, M.; Ali, S.; Ahmad, S.; Tasleem, S. Synthesis, characterization and advanced sustainable applications of titanium dioxide nanoparticles: A review. *Ecotoxicol. Environ. Saf.* **2021**, *212*, 111978. [CrossRef] [PubMed]
28. Marien, C.B.D.; Marchal, C.; Koch, A.; Robert, D.; Drogui, P. Sol-gel synthesis of TiO_2 nanoparticles: Effect of Pluronic P123 on particle's morphology and photocatalytic degradation of paraquat. *Environ. Sci. Pollut. Res.* **2017**, *24*, 12582–12588. [CrossRef]
29. Fessi, H.; Puisieux, F.; Devissaguet, J.P.; Ammoury, N.; Benita, S. Nanocapsule formation by interfacial polymer deposition following solvent displacement. *Int. J. Pharm.* **1989**, *55*, R1–R4. [CrossRef]
30. Islam, J.B.; Furukawa, M.; Tateishi, I.; Katsumata, H.; Kaneco, S. Photocatalytic degradation of a typical agricultural chemical: Metalaxyl in water using TiO_2 under solar irradiation. *SN Appl. Sci.* **2020**, *2*, 925. [CrossRef]
31. Memarizadeh, N.; Ghadamyari, M.; Talebi, K.; Torabi, E.; Adeli, M.; Jalalipour, R. Residues and dissipation kinetics of two imidacloprid nanoformulations on bean (*Phaseolus vulgaris* L.) under field conditions. *Pollution* **2019**, *5*, 871–878.
32. Chen, J.-Q.; Wang, D.; Zhu, M.-X.; Gao, C.-J. Photocatalytic degradation of dimethoate using nanosized TiO_2 powder. *Desalination* **2007**, *207*, 87–94. [CrossRef]
33. Nageswara Rao, T.; Prashanthi, Y.; Ahmed, F.; Kumar, S.; Arshi, N.; Rajasekhar Reddy, G.; Manohra Naidu, T. Photocatalytic applications of Fe–Ag Co-doped TiO_2 nanoparticles in removal of flumioxazin pesticide residues in water. *Front. Nanotechnol.* **2021**, *3*, 652364. [CrossRef]
34. Elsayed, E.; Hassan, H.; Abd El Raof, A.E.; Salman, S. Coupling Between Laser Irradiation and TiO_2 Nanoparticles on Efficient Decontamination of Some Pesticide's Residues from Orange and Tomato Puree. *Egypt. J. Chem.* **2021**, *64*, 971–979.
35. Loccufier, E.; Deventer, K.; Manhaeghe, D.; Van Hulle, S.W.; D'hooge, D.R.; De Buysser, K.; De Clerck, K. Degradation kinetics of isoproturon and its subsequent products in contact with TiO_2 functionalized silica nanofibers. *Chem. Eng. J.* **2020**, *387*, 124143. [CrossRef]
36. Nageswara Rao, T.; Hussain, I.; Anwar, M.S.; Koo, B.H. Photocatalytic degradation kinetics of pesticide residues in different pH waters using metal-doped metal oxide nanoparticles. *EQA-Int. J. Environ. Qual.* **2020**, *36*, 37–44.